Renal Cancer Cell Nuclei Detection from Cytological Images Using Convolutional Neural Network for Estimating Proliferation Rate

Md Shamim Hossain[1], Hamid A. Jalab[1], Fariha Zulfiqar[1], Mahfuza Pervin[2]
[1]*Faculty of Computer Science and Technology, University of Malaya, Kuala Lumpur, Malaysia*
[2]*Department of Horticulture, Bangladesh Agriculture University, Mymensingh, Bangladesh*
shamim4901@siswa.um.edu.my

***Abstract*— The Cytological images play an essential role in monitoring the progress of cancer cell mutation. The proliferation rate of the cancer cell is the prerequisite for cancer treatment. It is hard to accurately identify the nucleus of the abnormal cell in a faster way as well as find the correct proliferation rate since it requires an in-depth manual examination, observation and cell counting, which are very tedious and time-consuming. The proposed method starts with segmentation to separate the background and object regions with K-means clustering. The small candidate regions, which contain cell region is detected based on the value of support vector machine automatically. The sets of cell regions are marked with selective search according to the local distance between the nucleus and cell boundary, whether they are overlapping or non-overlapping cell regions. After that, the selective segmented cell features are taken to learn the normal and abnormal cell nuclei separately from the regional convolutional neural network. Finally, the proliferation rate in the invasive cancer area is calculated based on the number of abnormal cells. A set of renal cancer cell cytological images is taken from the National Cancer Institute, USA and this data set is available for the research work. Quantitative evaluation of this method is performed by comparing its accuracy with the accuracy of the other state of the art cancer cell nuclei detection methods. Qualitative assessment is done based on human observation. The proposed method is able to detect renal cancer cell nuclei accurately and provide automatic proliferation rate.**

***Index Terms*— Cell nucleus; Convolution neural network; Cytological images; Renal cancer.**

I. INTRODUCTION

Cancer is the most growing problem all around the world and it has become the primary cause of death. The main reason for cancer is the tumour cells and it is important to determine whether these cells are benign or malignant. Benign cells are the least aggressive and do not contain cancer cells. However, malignant cells have cancer cells and proliferate rapidly, which is the life-threating for the patients [1]. Renal cancer is the most common and aggressive cancer type among all others. Generally, the first step to detect the renal tumour is to use the medical reasoning images (MRI), which is then followed by performing the biopsy test. Biopsy test is the removal of small sample renal tumour tissue for diagnosis purpose by staining with dyes. Eosin and hematoxylin are the two stains to visualize the nuclei in terms of purple or blue color, while cytoplasm is in pink color to highlight the interesting point of the tissue. The pathologist finds the percentage of cancer cell proliferation rate and the result provides a better understanding for the physician to decide on the proper renal cancer treatment. According to the world cancer research fund, 80-90% of people are suffering from primary renal cancer disease [2]. If it is detected in the early stage and starts the treatment based on the accurate proliferation rate in the affected area, then it would not spread in the other area of the human body. The accuracy of the proliferation rate depends on the experience level and visual quality of the pathologist. While accuracy is an important issue because it is directly connected with the cancer treatment. However, it is difficult to detect the cancerous cell nuclei [3]. According to the American cancer society, approximately 70%-80% patients discover the renal cancer cell carcinoma at the 3rd or 4th stage, and in these stages, it is very rare to cure the patients excepts continuing the proper and accurate treatment based on the cancer proliferation rate until the patient's longevity [4].

Therefore, it is necessary for the medical professional to estimate the proliferation rate of cancer cell from the hundreds or thousands of samples of cytological images slide and observed the nuclei accurately which contains thousands of cells. Observation of the nuclei of the normal and abnormal cell is a time-consuming job. Sometimes, pathologist lost the concentration, and according to the visual appearance, many abnormal nuclei are similar to the normal nuclei. So, it is essential to building a machine-oriented automated detection process to detect the nuclei from the renal cancer cell as well as the detection of nuclei from other cancer cells. However, it is very challenging to develop an automated and efficient nuclei detection process and measure the proliferation rate based on the renal cancer cell histopathology images due to the complex structure of histopathological images.

In general, reasons for the increase complexity to detect the nuclei from the cell are such as the large number of nuclei and high resolution of pathology images. Additionally, the cell structure, namely the different size, shape, texture and appearance of an individual nucleus also contribute to the difficulties to detect the nuclei. The touching and overlapping cells are the primary difficulties for machine-based nucleus segmentation and detection. Besides, the boundary of the touching and overlapping cells

are not as smooth as an isolated nucleus. Another important factors are the non-homogenous and noisy background.

Therefore, automated cancer cell diagnosis and prognosis is crucial in the pathological department to assist the pathologist in detecting the abnormal renal cancer cell nuclei automatically from the cytoplasmic image of cancer affected area. This approach can eventually lead to accurate identification for anti-cancer treatment. The rest of the study is arranged as follows. In section II, the related works of the nucleus detection of the cell are briefly explained. The proposed hierarchical R-CNN method and procedure are described in part III. The experimental results of the proposed process and comparison with the other existing methods presented in section IV. Finally, section V draws the conclusion by pointing out further works of the proposed method.

II. Literature Review

Researchers have focused their interest in the field of automated cancer cell diagnosis because of the necessity for accurate nucleus segmentation and detection. Several computer-based methods have been implemented in the past few years. In general, these methods are divided into three steps: cell segmentation to detect the nucleus, extraction of the nucleus features and then classification of the normal and abnormal nuclei. Some methods are semi-automated, while others are automated. However, the basic idea is to extract the structural information of the cell such as the shape, texture, staining intensity and number from an individual cell. Among all these methods, artificial intelligence and deep learning neural network approaches have achieved satisfactory results and have been applied in cell detection and segmentation for classifying the normal and abnormal nuclei. However, despite the progress of recent detection methods, the accurate nucleus detection of the cancer cell is a challenging task because of reasons such as weak contrast, diffused background, touching and overlapping of nuclei and irregular nuclei shape. Therefore, up till now, accuracy detection of the nuclier is not at its satisfactory level [5].

The cancer cell and nucleus detection are classified into two categories:

i. The threshold-based segmentation with the morphological operation, region growing, level sets, graph-cuts and k-means clustering.
ii. The deep learning models for image segmentation with the deep neural network.

Kun Zhang et al. [6] proposed a framework where colorectal cancer cells are automatically detected. While Mandal et al. [7] presented a method with naïve Bayes, logistic regression and decision tree. Logistic regression is used to extract the nucleus features as well as select the features. Naïve Bayes classifier is designed based on the Bayes' theorem, and it is used to predict the probability of class membership and decision tree that supports the class of normal and abnormal nuclei. Veta et al. [8] proposed a method, where the nucleus centre is identified by the direction of the gradient, but this method does not able to detect the irregular shape and spindle shape nucleus. Vink et al. [9] used ADA-boost classifier for training the two detectors. One is the Haar-like features, and another one is the pixels-based features, in which both detectors are merged for the purpose of the training. After that, this combined detector is applied to the histopathology stained breast cancer cell images. The performance of this method is very poor when small nuclei and thin fibroblasts are detected. Sharma et al.[10] proposed a segmentation method for nucleus detection based on text feature, morphological and intensity with ADA-boost classifier. This work can only detect the nucleus, but it cannot classify the normal and abnormal cell. Chung et al. and Zheng et al. [11, 12] implemented superpixels and support vector machine (SVM) to detect the normal and abnormal nuclei of the tumour tissue. In these two methods, the (SVM) classifier are trained to achieve the segmentation results. However, the segmentation process is time-consuming, and the detection of the cell with a weak edge is relatively poor. Alomari et al.[13] proposed a method where the pathology image is divided into six patches and applied threshold value to find the density of the pixels from every patch. After that, the bounding box is used to localise the nuclei. The evaluation result of this method is 84% accurate. Next, Alomari et al. [1] introduced an improved method by segmenting the nuclei based on colour features with k-means clustering of stained histopathology images. The cancerous cell is represented by the brown cell, and the normal cell is represented with the blue cell. Then, the circularity features are used to count the nuclei of the cancerous cell to estimate the proliferation rate. George et al.[14] presented a remote computer-aided breast cancer cell detection method, where the location of the nucleus is detected with Hugo Transformation. The blood cell, noisy circle and other false positive are removed by the fuzzy c-means clustering and Otsu's threshold. After that, the segmentation of nuclei boundary is performed with marker-controlled watershed transformation. At last, the probability neural networks are used for the classification of nucleus and accuracy is 90.99%.

Recently, deep neural network based methods has provided better results than the segmentation based methods as they have been able to deal with a large number of histopathological images. Song et al. [15] proposed a deep learning method and a deformation model to detect the cervical cancer cell. Convolution neural network is used to learn the cell feature to classify the nucleus, cytoplasm and background. After that, overlapping cells are split based on the shape of cells using Gaussian kernel fitting. Next, Song et al., and Zhang et al. [16, 17] introduced an improved method, where cytoplasm and nucleus are segmented with multi-scale convolution network (MSCN) and graph partitioning method. Firstly, the cell features are detected with the MSCN, and then this harsh segmentation is refined with the graph partition method based on pre-learning nucleus features. The overlapping nuclei are segmented with nuclei clump splitting algorithm. However, these methods cannot detect the isolated nucleus and overlapping nuclei in the same process. In the recent work of Song et al. [18], the overlapping nuclei as well as an isolated nucleus are segmented from the cervical cancer tissue during the same process. In this method, the cost function is used to segment the overlapping nuclei, and then the edges of the nuclei are refined with the dynamic multi-template nucleus shape

model. Deep convolution network is used to learn the different shapes of the nucleus. This method also can detect the nuclei, that have weak or lost boundary for overlapping. Malon et al.[19] used the convolutional neural network (CNN) to classify the non-mitotic and mitotic cell based on the shape information, texture and colour features. Wang et al. [20] presented a cascade classifier, which is the combination of the hand-crafted features. The features are learned with CNN to detect the cancer nucleus. Two-stage cascade CNN is proposed by Hu et al.[21], where CNN network is trained with the cancer cell patches which are detected with the selective search instead of using region of interest (ROI). In this method, the cancer cells are processed after the detection of selective search and before feeding them as input to CNN. However, this method is challenged due to its low contrast histopathological images. Cruz-Roa et al. [22] applied deep learning method with pre-defined bag of features and discrete wavelength transformation to detect the basal-cell carcinoma. To detect the nucleus, Xu et al. [23] proposed stacked sparse auto-encoder to learn the regions of the nuclei of cell in an unsupervised way and soft-max classifier is employed to classify non-nucleus and nucleus objects. This method is applied to the 500 histopathology images of breast cancer and the accuracy is 84.49%. Ciresan et al. [24] detected the nuclei of the mitotic breast cancer cell with CNN, which is learned with the probability pixels that belong to the mitotic nucleus pixels. Each mitotic nucleus patch is taken based on the centre of probability pixels. Xie et al. [25] proposed a method where the nuclei patches are learned with structural regression CNN and the patches are selected based on the voting scheme, where the centre of nucleus exists. Moreover, Xie et al. [26] introduced an improved structured regression method with fully residual CNN. This model is learned to create a compact proximity map at the higher response around the cell centre instead of the patch classification. The structure information of the cell is encoded, and the pixels that are near to the cell centre achieved more values than the neighboring pixels. However, the performance of this method is inefficient in a large number of cells in the cytoplasmic image, irregular shape of the cell and non-homogenous background noise. Ma et al. [27] presented a cell detection method for head and neck cancer cell, where the method is divided into three steps: pre-processing, patch extraction and convolution neural network to learn the features. In the pre-processing step, cell images are normalized to eliminate the dark reference. However, it also eliminates the essential pixel attributes of the cell. In patch extraction, features are extracted from the patch as a pixel vector for training and these features are fed as input for CNN. However, the nucleus detection accuracy is 86.05%, and this accuracy affects the proliferation rate. Another histopathology image analysis using deep learning for non-small cell lung cancer is presented by Nicolas et al. [28]. In this method, each layer of CNN is trained with cell features without any pre-processing. Instead of training all the layers, only the last layer is trained as a transfer learning, and the accuracy is 92%. Zhang et al. [29] proposed a pre-trained neural network. The cervical cancer nuclei are fine-tuned and resampled in the last layer, which is the main advantage of transfer learning approach. The performance of this method is 91.3%. However, it uses pre-trained network, which is not efficient to detect other cancer cell nucleus. Chandran et al.[30] introduced a semi-supervised deep learning neural network. In this method, the patches of retinal cancer cell are segmented with three modules. In the first module, the maximum and minimum pixel values are set and sent it to the second module to calculate the similarity of pixel values. In the third module, complexity is measured, and the segmented patches are fed as input for the deep learning neural network (DLNN). But the threshold value is predefined, in which it is adjusted according to the histopathological images. Therefore, the accuracy of the nuclei detection depends on a suitable threshold value, which is not efficient. Spatially constrained convolution neural network (SC-CNN) is proposed by Sirinukunwattana et al.[31]. In this method, each nucleus is a collection of pixels, and this method finds the probability of the pixel of being nucleus pixel using neighboring ensemble predictor (NEP). The NEP measures the probability based on the intensity value of nucleus pixels. The higher probability of the nucleus center is indicated with the higher value of pixel. After segmenting the colon cancer nucleus, all the nuclei patches are trained with the CNN. This method can accommodate a large amount of training data. However, NEP not only detects the cancer cell nucleus but also detects the normal cell nucleus, which has a similar probability. Therefore, the probability value is adjustable, and this value is set within a suitable range to find a better result. In this method, probability value $M = 2$ is taken for the experimental purpose. Xing et al. [32] introduced a method where the nuclei patches are cropped with a sliding window method. Then, the patches are learned with CNN to create a probability map. The larger probability of input patches belongs to the nuclei of the cancer cell. After that, the nuclei shapes are marked with the iterative region merging algorithm and all overlapping nuclei are detected with H-minima transformation. Li et al. [33] applied the granularity and morphological process to detect blood cancer cell object. Granularity process with probe structure is analyzed based on the smooth and noiseless image. After that, morphological operation-erosion and dilation are employed. Four features of rectangular factor, area, roundness and elongation of the cell are considered for the segmentation with the adapted active contour algorithm. However, this process is iteratively applied to find the optimal segmentation results leading to an increase in the processing time and a rise in the over segmentation results. Granularity process is also used by Narayanan et al. [34], and for the final cell segmentation, stochastic gradient optimizer is used. After that, constrained CNN are applied to classify the cancer cell nuclei. A supervised model combined with deep learning and handcrafted features is proposed by the Saha et al.[35], in which the textural, intensity and morphological features are known as handcrafted features. In this method, the rectified linear unit (ReLU) is applied after every convolution layer and dropout layer is added to reduce the overfitting difficulty after the final connected layer. However, the precision rate is 92%. Feature-based cell segmentation is used by Khoshdeli et al.[36]. In this method, the Laplacian of Gaussian (LoG) filter is applied to extract the cell shape. The colour decomposition information is also

provided by the LoG filter. After that, CNN is combined with the LoG response and applied to detect the nucleus.

Based on the above approaches, the high efficiency and accurate results are provided with the combination of classifying segmented regions approach followed by the convolutional neural network method to detect the nucleus in the histopathology image are mostly for separating the normal and abnormal nuclei. In the proposed method, the renal cytoplasmic image regions are segmentated with the k-mean clustering based on color features to detect the object regions and non-object regions. After that, the object regions are determined with the SVM whether it is normal or abnormal cell nuclei. Selective search is applied to separate the isolated and touching or overlapping cell nuclei. Finally, regional convolutional neural network (R-CNN) is trained with normal and abnormal cell nuclei to detect the renal cancer cell nucleus, which is able to estimate the proliferation rate accurately. The performance of the proposed method is outstanding no matter whether it involves with the touching or overlapping cell and the number of the clustered cell.

III. PROPOSED METHOD

To detect the renal cancer cell nucleus efficiently and measure the proliferation rate accurately, the hierarchical method is proposed. The proposed method is divided into four steps and organized as follows: cell region segmentation, cell region classification, touching or overlapping cell identification, and the learning normal and abnormal cell regions and proliferation rate estimation. The workflow of the proposed method is presented in Figure 1.

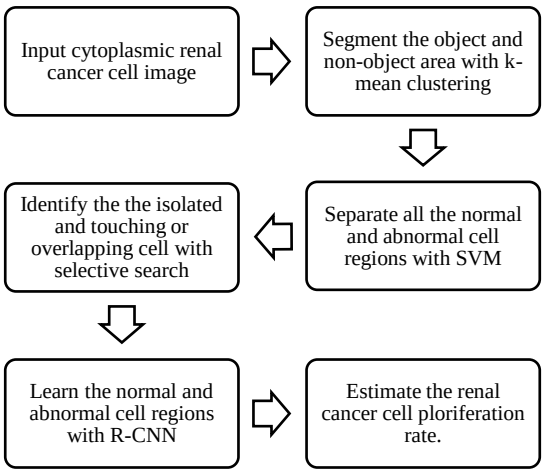

Figure 1: The hierarchical framework of renal cancer cell nucleus detection and proliferation rate estimation

A. Cell Region Segmentation

The aim of the cell region segmentation is to classify the pixels of the cell region and complex background. Each cell is represented by a single nucleus. Thus, the cell segmentation is very critical because of noise. The K-mean clustering is applied to remove all the uniform areas, such as background based on different color features. The feature channel is extracted from the L*a*b color model. L*a*b color model is very efficient for decoupling of color and intensity [1].

$$L^* = 116\left(\frac{M}{Mx}\right)^{1/3} - 16 \quad (1)$$

$$a^* = 500\left[\left(\frac{N}{Nx}\right)^{1/3} - \left(\frac{M}{Mx}\right)^{1/3}\right] \quad (2)$$

$$b^* = 200\left[\left(\frac{M}{Mx}\right)^{1/3} - \left(\frac{I}{Ix}\right)^{1/3}\right] \quad (3)$$

where: L = The brightness
a* = The ratio of green-red color
b* = The ration of blue and yellow color

The L*a*b color model image is presented in Figure 2. The original image is modified based on the L*a*b color model. The brown cell is clustered after segmentation. The brown cells are converted to light brown cells by taking the low value of L. This modification improves the clustering performance and reduces the loss of information, as shown in Figure 3.

The a* and b* channels are used for the color features of the K-mean clustering to classify the background and cell regions. The image is grouped into two clusters: tissue background and nucleus. After that, the image is converted into a greyscale image to perform canny edge detection. The holes appear in some cells. These holes are required to be filled to detect the boundary of the cell regions with canny edge detection. Therefore, the morphological operation is applied to fill the hole, as shown in Figure 4. After that, the image is ready for used as input of the support vector machine [12].

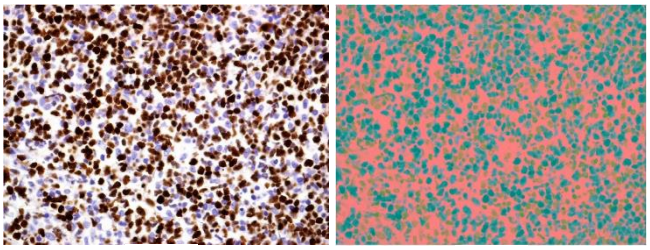

Figure 2: The example of L*a*b image; (a) the original image; (b) after L*a*b image transformation

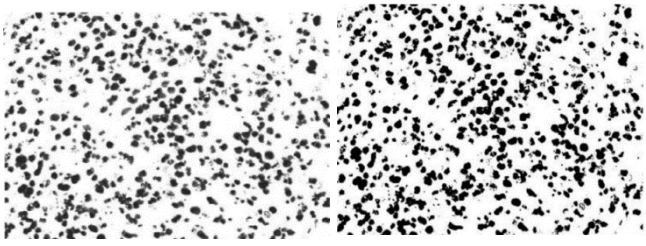

Figure 3: The example of a segmented image; (a) the brown cells image; (b) the blue cell image

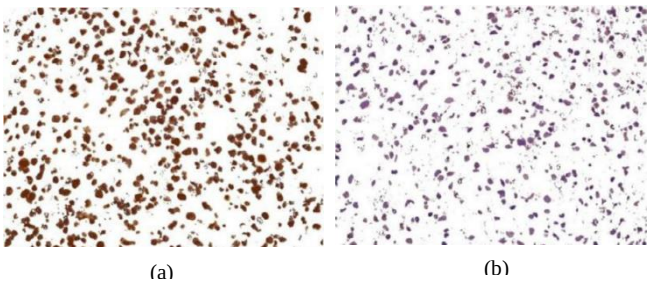

Figure 4: The example of morphological operation; (a) the grayscale image; (b) image after dilation

B. SVM To Classify Cell

The SVM has an excellent capability to classify with the small amount of training data samples. An SVM is trained with a label and the feature vector to classify the nucleus region. The sample training image is labelled manually. After that, the hyperplane among the classes is maximized with the SVM. The idea of SVM is explained as follows [12]:

Suppose, training data is $\{x_i, y_i\}_{i=1}^{S}$, where, the feature vector is defined as x_i, the binary label which indicates the cell region is defined by $y_i = \pm 1$, the size of samples training data is determined as S, where, $i=1, 2, 3, ...S$. Therefore, the decision support function is defined as:

$$f(x)=\text{sgn}\left(\sum_{i=1}^{S} a_i^* y_i K(x_i,x)+b^*\right) \quad (4)$$

where, a_i^* is the Lagrange multiplier and the bias b^*, which is learned from the samples of training data. The kernel function is defined as $K(x_i,x)$,which is used to find the relationship between x (feature vectors) and x_i (support vector). To find the optimal value of a_i, the Lagrangian value is minimized under the constraints and is defined as:

$$\sum_{i=1}^{S} a_i y_i=0, \quad 0\le a_i \le C \quad (5)$$

$$W(a)=\sum_{i=1}^{S} a_i-\frac{1}{2}\sum_{i=1}^{S}\sum_{j=1}^{S} a_i a_j y_i y_j K(x_i,x_j) \quad (6)$$

where the penalty parameter C is manually specified. However, the larger value of C is the higher penalty for misclassification. It is required to define the kernel function $K(x_i,x)$ for SVM. In general, the linear kernel, radial kernel and polynomial kernel function are applied for SVM. In the proposed method, the radial kernel is applied, and the equation of redial kernel is defined as:

$$K(x_i,x_j)=\exp(-\lambda \| x_i-x \|^2) \quad (7)$$

where λ is defined as a regularization parameter. This parameter is adjusted to find the optimal classification result [34].

C. Selective Search For Irregular Cell

Selective search is a region proposal algorithm and design for fast recognition of the object location with high recall. It is used for grouping of similar areas of the image, such as texture, color, shape compatibility and size. After accurately separate the nuclei regions, the overlapping nuclei are observed because of their irregular nuclei shape.

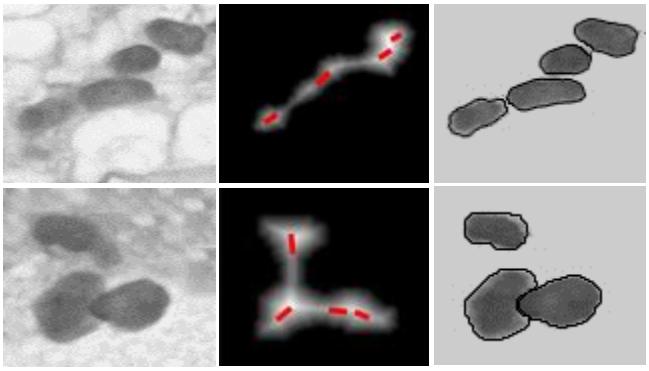

(a) (b) (c)

Figure 5: The example of splitting nuclei; (a) touching and overlapping images; (b) internal distance map; (c) split lines are surrounded at each nucleus.

To detect the overlapping segmented nuclei, the marker-based splitting algorithm is used in the proposed method. The touching nuclei are identified based on the number of markers, as shown in Figure 5. The number of markers determines whether the overlapping nuclei exist or not [32].

Based on the observation, the shape of the renal cancer cell nuclei is convex, and each nucleus object has the local distance from cell nuclei boundary. The local distance of the overlapping nuclei has the maximum distance. Hence, the distance transformation map from the centre of the nucleus is used to calculate the number of markers. The inner-distance of the nucleus is defined as [16]:

$$D(p)=\min_{q\in E} \| p-q \| \quad (8)$$

where p is the nucleus pixel, $\| \bullet \|$ is defined as the Euclidian distance, and q is defined as the element of an edge pixel of the nucleus boundary.

To detect the marker of overlapping nuclei, the present pixel value should be greater than or equal to the neighbor pixels values within the 3×3 regions. To mitigate the noisy pixel impact, the threshold value T is set and defined as [16]:

$$T=\mu M(p)-(\max_{i\in M} D(i)+\min_{i=M} D(i)-2M(p)) \quad (9)$$

$$M(p)=\frac{1}{N}\sum_{i\in M} D(i) \quad (10)$$

where, μ is defined as adjustment parameters, M is defined as the collection of markers, N is defined as the amount of pixels i to the M. Therefore, if the value of T is greater than the marker distance, then it would be discarded. According to the observation, the single nucleus may have several markers and should be combined into one marker. However, the total number of markers is unidentified. Therefore, the clustering method is implemented to combine with the geometrical information to increase the precision of markers. In the evidence distance of the m_i and m_j, markers are measured with the clustering effects and defined as [16]:

$$g(m_i,m_j)=\min_{p\in m, q\in m_j} \| p-q \| \quad (11)$$

Instead of a grid search or hard threshold, the adaptive threshold is used and defined as [16]:

$$g(m_i, m_j) = \min_{p \in m, q \in m_j} \| (D(p) - D(q)) \| \quad (12)$$

In conventional clustering, the overlapping nuclei may have lost the distance information because of the cluster centre is used for creating the new cluster. Therefore, the original marker is remained, and the clusters of pixel classes m_i and m_j are combined to create a new cluster, as shown in Figure 5. The new cluster is not able to generate the further cluster since the current distance is not the local-maxima. Consequently, the new marker is not able to represent the single nucleus object. As a result, the splitting error occurs with unnatural nucleus boundary. This problem is solved by keeping the original distance information.

After getting the appropriate makers, the nearest neighbor assignment is used to determine the split border of the touching nuclei, and the nearest marker is assigned for each pixel. However, the unnatural nucleus boundary is created for more variation of nucleus size. The effective evidence is measured from the marker pixel to solve this problem. Suppose, $L(p, m_i)$ is defined as the effective evidence from pixel p to marker m_i and is determined as [16]:

$$L(p, m_i) = \eta \| D(p) - \min_{q \in m_i} D(q) \| + \nu \| I_p - \overline{m_i} \| \quad (13)$$

where I_p is defined as the mean intensity of 5×5 patch, which is centred at p. $\overline{m_i}$ is defined as the average intensity of the marker m_i of inner-distance and η, ν are defined as the adjusting parameters. After that, the p is defined as:

$$S(p, m_i) = \arg\min_{m_i \in \text{markers}} L(p, m_i) \quad (14)$$

D. R-CNN To Detect The Cancer cell

R-CNN is a deep neural learning architecture consisting of non-linearity, convolutional (Conv), pooling (pool) and fully connected layers (f_c). The raw segmented nuclei pixels are taken as input to train the ConvNet. The output layer is the combination of several neurons, which represents the single class. The weight (W) of the neural network is optimized using the backpropagation method by reducing the classification error of training sets. Detected renal cancer cell nuclei are trained with ConvNet, as shown in Figure 6 [36].

The patches of segmented nuclei as input and convolution filter are applied. The sum of Conv is taken as input for the non-linearity function, where the rectified linear unit (ReLU) $f(x) = MAX(0, x)$. The similar filter is used for the same features map. The filter is not the same for the different features. The same pattern of feature map in different regions is detected by the sharing property of the filter in the convolution layer. The feature response of each patch is down-sampled and summarized in the pooling layer and often estimates the maximum pooling (max-pooling). This layer is also responsible for the mirror translation of the nucleus. The features maps are combined in the first several layers and sent to the feature vector. The last layer of f_c consists of two neurons, which are used to detect the abnormal and normal nuclei. The dropout is applied to decrease the overfitting in the fully connected layers. The weights of ConvNet are updated according to the gradient of the loss function. The learning rate is gradually reduced after a few epochs. The learning process is stopped after the number of pre-determined epochs [29]. The Conv and pool layers generate the small patches and pass through the f_c layers. The proposed R-CNN architecture consists of six Convolution layer, five max-pooling layer, five ReUL and two full connected final layers, as shown in Table 1. At the initial stage, three feature maps are taken where the filter size is 2×2. In the first and second layer, the number of feature maps is the same, but the number of neurons is reduced to 35×35, where the filter size is 4×4. In the fourth layer, the filter size is 3×3. After that, the filter size is 2×2 for all the layers until the fully connected layer, where filter size is 1×1. The filter is moved on the feature map; therefore it is important to reduce the filter size to increase the feature map to provide more information in the fully connected layer. The dropout is assigned to 0.05 for improved learning result. The workflow and the overall process of nuclei detection are presented in Figure 6 [35].

Table 1
Neural Network Architecture

Layer	Type	Maps	Neurons	Filter size
0	Input Image	3	71x71	2x2
1	Conv	90	70x70	2x2
2	Max-pooling	90	35x35	4x4
3	Conv	256	32x32	2x2
4	Max-pooling	256	16x16	3x3
5	Conv	384	14x14	2x2
6	Max-pooling	384	7x7	2x2
7	Conv	512	6x6	2x2
8	Max-pooling	512	3x3	2x2
9	Conv	512	2x2	2x2
10	Max-pooling	512	3x3	2x2
11	Conv	512	2x2	2x2
12	Fully Connected (f_c)	-	1000	1x1
13	Fully Connected (f_c)	-	2	1x1

E. Proliferation Rate

The last step of the proposed method is the estimation of the proliferation rate. The simple statistical calculation is performed to measure the proliferation rate of the abnormal cell which helps the pathologist to determine the aggressiveness of renal cancer cell. The proliferation RATE(pre) is defined as [1]:

$$PRE = \frac{\text{Numberof abnormalnuclei}}{(\text{Numberof abnormalnuclei} + \text{Numberof normalnuclei})} \quad (15)$$

IV. EXPERIMENTAL RESULTS

The proposed method is implemented using Matlab 2018a. The microscopic cytoplasmic images of renal cancer cell are publicly available for research purpose [33]. All the images from pathology slides are taken with Aperio Digital Pathology Slide Scanners (model CS2). It allows to view the ultrastructure of each cell with bright field illumination where magnification is 40x: 0.25µM/pixel and scan method

is time delay and integration (TDI) line scan. The average tissue thickness is (3-5 µm), where the tissue is stained with hematoxylin to increase the cell contrast. The sample slide images of 33 patients are taken, and total samples are divided into five sets to reduce the training time. These microscopic image data sets are available and open for research purpose [37].

The proposed method is tested on the renal cancer cell data sets. The accuracy of the proposed method to detect the abnormal nucleus from the cytoplasmic image is compared with the existing methods using the same data sets.

The performance of the neural network is mostly depended on the parameter values, such as the number of hidden layers, Root Mean Square Error and Correlation Coefficient (R-value) between the targets and the outputs. Before starting the training, several parameters are initialized, such as the total number of test iteration, training and validation batch sizes etc. The 16,905 segmented cancer cell and 22,948 normal cell nuclei of sample images are taken as training patches (t_s), and 4,217 patches are taken as validation patches (v_s). The size of the training batch is the total number of patches processed in one batch.

In the proposed R-CNN, the batch size (t_b) is assigned to 256. The validation batch size v_b is the total validation patches processed in the test phase and v_b is assigned to 50. The testing iteration ts_{it} is measured as: $ts_{it}=(v_s / v_b)$.

The testing interval ts_{iv} is calculated by the number of validation of the proposed method and ts_{iv} is assigned to 5,000. Therefore, (t_s / t_b) iterations are required to complete the single epoch or whole training set. The maximum iteration is assigned to 300,000; learning rate is assigned to 0.01, weight decay is assigned to 0.005 and momentum is assigned to 0.9[35].

A. Qualitative Evaluation

The limitations of overlapping nucleus have been overcome by properly stained the sample slide. Moreover, the complicated shape of overlapping nuclei can degrade the segmentation results. Therefore, the features of the overlapping cell are extracted and t-test is performed. The visualization of the filter layer and the feature training layer are shown in Figure 6. The features maps are presented in the hidden layers. The architecture of the proposed method is created with these features maps and allows to detect the abnormal nuclei from the sample image. The qualitative results of the proposed method are presented in Figure 7.

According to the output of the proposed method, the abnormal cells are represented with the yellow circle, and the normal cells are represented with the red circle. Therefore, according to the visual observation, the better detection result is provided with the proposed method.

B. Quantitative Evaluation

The proposed method is quantitatively evaluated with the precision (PR), recall (RC) and F-measurements (FM).

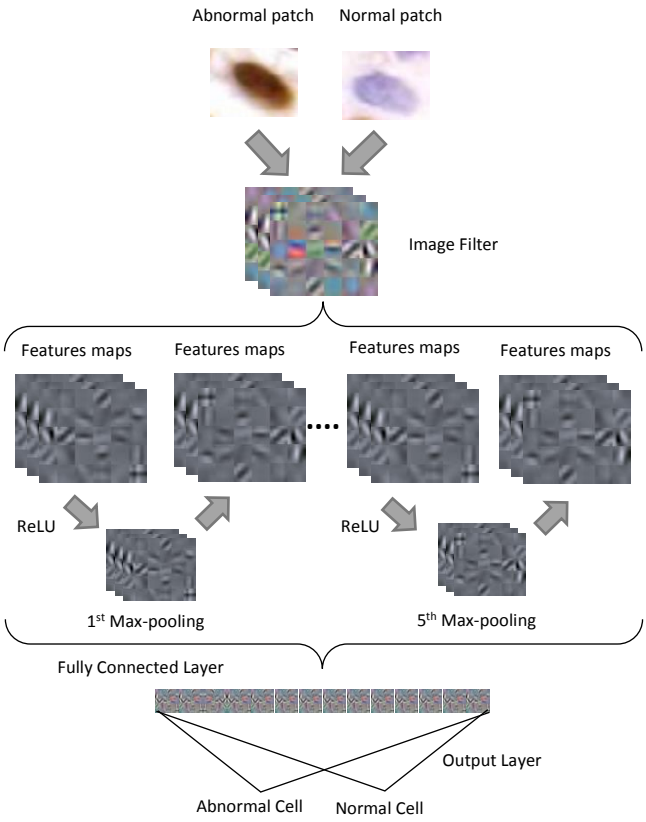

Figure 6: The example of the workflow of the R-CNN network

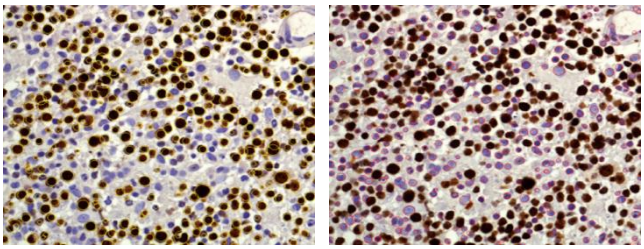

Figure 7: The example of the detection output of the proposed method; (a) the abnormal cell detection; (b) the normal cell detection

This method is compared with the existing methods and abnormal nuclei detection with the histology expert.

$$P = \frac{TP}{TP + FP} \tag{16}$$

$$r = \frac{TP}{TP + FN} \tag{17}$$

$$f = \frac{2}{(1/PR + 1/RC)} \tag{18}$$

$$\rho = \frac{x - y}{\sigma / \sqrt{n}} \tag{19}$$

The data set is divided into five sets, and each set contains 10 sample images. For every set, the true positive (TP) is measured. The TP is defined as the agreement for the abnormal nucleus detection between the proposed method and histology expert. The false positive (FN) happens when the histology expert is able to detect the abnormal nucleus, but the proposed method fails. The false positive (FP) occurs when the proposed method is able to detect, but the expert fails to detect the abnormal nucleus. The precision

(PR), recall (RC) and F-measurement (FM) are calculated for each set and presented in Table 2 and 3 [1].

Table 2
Blue Cell Detection With Proposed Method

Set	MC	PC	TP	FN	FP	PR	RC	FM
1	3466	3457	3432	34	25	99.2%	99.0%	99.2%
2	5319	5427	5273	46	154	97.1%	99.1%	98.0%
3	4753	4755	4628	125	127	97.3%	97.3%	97.3%
4	4004	4029	3965	53	63	98.6%	99.1%	98.8%
5	5793	5728	5646	93	82	98.5%	97.4%	97.9%
Total	23335	23389	22948	351	441	98.1%	98.3%	98.2%

MC = Manual count, PC = Proposed method count, TP = True positive, FN = False positive, FP = False positive, PR = Precision, RC = Recall, FM = F-measurement

Table 3
Brown Cell Detection With Proposed Method

Set	MC	PC	TP	FN	FP	PR	RC	FM
1	4902	4860	4826	76	34	99.3%	98.4%	98.8%
2	3781	3782	3754	27	28	99.2%	99.2%	99.2%
3	2619	2610	2591	28	19	99.2%	98.9%	99.0%
4	3917	3878	3841	76	37	99.0%	98.0%	98.4%
5	1911	1922	1893	18	29	98.4%	99.0%	98.6%
Total	17130	17052	16905	225	147	99.0%	98.7%	98.8%

MC = Manual count, PC = Proposed method count, TP = True positive, FN = False positive, FP = False positive, PR = Precision, RC = Recall, FM = F-measurement

According to the statistical data of Table 2, the accuracy of the proposed method for normal (blue) cell detection is, PR = 98.1%, RC = 98.3% and FM = 98.2%. The accuracy of the abnormal (brown) cell detection for the proposed method based on the Table 3 statistical data is, PR = 99.0%, RC = 98.7 % and FM = 98.8. The proposed method outperforms at any condition of the stained cytoplasmic image. The sample outcome results are shown in Figure 7, and the performance of the proposed method is very accurate for overlapping nuclei.

In addition, in equation (19), the mean value of two samples is defined by x and y. The difference between the two samples is defined with the standard deviation σ, and the sample size is denoted as n. However, if P is less than the significant value 0.05, these samples are considered as statistically significant. However, the proper abnormal nuclei detection and the accurate proliferation rate are achieved with the proposed method [35].

C. Comparison With Other Methods

To evaluate the performance of the proposed method, experimental comparison has been implemented with the existing methods. The same data sets were used for the other different nucleus detection methods and the value of PR, RC and FM are presented in Table 4. The same validation procedure was employed for all the existing methods.

The manual observation of detecting abnormal nuclei was done by the pathology expert. In general, the proposed method is very close to the manual proliferation estimating value. The proposed method is able to detect the overlapping nuclei within a fixed range as well as the irregular shape nuclei. The performance of the CHT method is intermediate, whereas the IRIC method is remarkably better than the other existing methods; however, the performance is poor for the overlapping nuclei. The limitation of RCD method is unable to detect the irregular shape nuclei. However, the average training time of the R-CNN for 30 epochs is 4 hours. Therefore, the computational time of the proposed method is faster than the existing techniques and suitable to be used for clinical applications. According to the classification strategy $N_v \times N_c = 1000$, the average testing time for the single renal cancer cell nucleus is 3.5 seconds.

Table 4
Comparison With Existing Methods

Methods	Precision	Recall	F-measurement
Circular Hough Transformation Method (CHT)[38]	69.52%	61.93%	65.56%
Area morphological Method (AM)[39]	83.55%	66.23%	79.42%
Cascaded Mitosis Detection method (CMD)[20]	84.27%	65.72%	73.60%
Deep learning Based Method (DLB)[40]	88.48%	70.53%	78.11%
Iterative Structural Circular Detection Method (IRIC)[1]	92.46%	88.31%	90.70%
Handcrafted Featured Deep Learning Method (HFDL)[35]	97.75%	98.01%	97.31%
Proposed method	99.01%	98.70%	98.8%

V. Conclusion and Future Work

The cancer proliferation rate is important for appropriate the dosing of the right anti-cancer drug and the prediction of drug response for the cancer cell. It is also an indicator to prognosis the aggressiveness of the cancer cell. The manually abnormal cell observation is a very monotonous work for the pathologists, and accurate proliferation estimation is a great challenge for them. The proposed method is introduced to reduce the time and improve the accuracy of the proliferation value as well as assist the pathologists to analyze the cytological images.

This method decreases the number of parameters of the R-CNN architecture, as it only needs to set the value of minor parameters. The several comparisons with the existing work demonstrate the better performance of the proposed method. On the other hand, the segmentation accuracy is ensured by the SVM. The touching and overlapping nuclei detection are enhanced with the proposed method to detect the irregular shape nuclei and stained in different conditions. Apart from this, the misclassification as abnormal cell nuclei is reduced.

The internal information of each cytoplasmic image can also carry valuable information about the disease. Therefore, it is also required to identify the irregular spot of the image to help the pathologist to predict the disease factors. The computational time would be significantly improved if the segmented nucleus is in the proper size for input as R-CNN. The poor quality of the nucleus region is the critical factor for the R-CNN. Therefore, the quality of the nucleus region would be improved in future work.

REFERENCES

[1] Y. M. Alomari, S. N. H. S. Abdullah, R. R. M. Zin, and K. Omar, "Iterative randomized irregular circular algorithm for proliferation rate estimation in brain tumor Ki-67 histology images," *Expert Systems with Applications*, vol. 48, pp. 111-129, 2016.

[2] S. I. Ferlay J, Ervik M, Dikshit R. (2015). *Kidney cancer statistics*. Available: https://www.wcrf.org/int/cancer-facts-figures/data-specific-cancers/kidney-cancer-statistics

[3] P. Weissleder, Nam JM, Thaxton CS, Mirkin CA. (2017). *Earlier Detection and Diagnosis*. Available: https://www.cancer.gov/sites/nano/cancer-nanotechnology/detection-diagnosis

[4] L. J. Clague J, Cassidy A,. (2017). *Early Detection, Diagnosis, and Staging*. Available: https://www.cancer.org/cancer/kidney-cancer/detection-diagnosis-staging/detection.html

[5] W. William, A. Ware, A. H. Basaza-Ejiri, and J. Obungoloch, "A review of Image Analysis and Machine Learning Techniques for Automated Cervical Cancer Screening from pap-smear images," *Computer Methods and Programs in Biomedicine*, 2018.

[6] K. Zhang *et al.*, "Multi-scale Colorectal Tumour Segmentation Using a Novel Coarse to Fine Strategy," in *BMVC*, 2016.

[7] S. K. Mandal, "Performance Analysis Of Data Mining Algorithms For Breast Cancer Cell Detection Using Naïve Bayes, Logistic Regression and Decision Tree," *International Journal Of Engineering And Computer Science*, vol. 6, no. 2, 2017.

[8] M. Veta, P. J. Van Diest, R. Kornegoor, A. Huisman, M. A. Viergever, and J. P. Pluim, "Automatic nuclei segmentation in H&E stained breast cancer histopathology images," *PloS one*, vol. 8, no. 7, p. e70221, 2013.

[9] J. Vink, M. Van Leeuwen, C. Van Deurzen, and G. De Haan, "Efficient nucleus detector in histopathology images," *Journal of microscopy*, vol. 249, no. 2, pp. 124-135, 2013.

[10] H. Sharma *et al.*, "A Multi-resolution Approach for Combining Visual Information using Nuclei Segmentation and Classification in Histopathological Images," in *VISAPP (3)*, 2015, pp. 37-46.

[11] H. Chung, G. Lu, Z. Tian, D. Wang, Z. G. Chen, and B. Fei, "Superpixel-based spectral classification for the detection of head and neck cancer with hyperspectral imaging," in *Medical Imaging 2016: Biomedical Applications in Molecular, Structural, and Functional Imaging*, 2016, vol. 9788, p. 978813: International Society for Optics and Photonics.

[12] X. Zheng, Y. Wang, G. Wang, and J. Liu, "Fast and robust segmentation of white blood cell images by self-supervised learning," *Micron*, vol. 107, pp. 55-71, 2018.

[13] Y. M. Alomari, S. Abdullah, S. N. Huda, R. R. MdZin, and K. Omar, "Adaptive localization of focus point regions via random patch probabilistic density from whole-slide, Ki-67-stained brain tumor tissue," *Computational and mathematical methods in medicine*, vol. 2015, 2015.

[14] Y. M. George, H. H. Zayed, M. I. Roushdy, and B. M. Elbagoury, "Remote computer-aided breast cancer detection and diagnosis system based on cytological images," *IEEE Systems Journal*, vol. 8, no. 3, pp. 949-964, 2014.

[15] Y. Song *et al.*, "A deep learning based framework for accurate segmentation of cervical cytoplasm and nuclei," in *Engineering in Medicine and Biology Society (EMBC), 2014 36th annual international conference of the IEEE*, 2014, pp. 2903-2906: IEEE.

[16] Y. Song, L. Zhang, S. Chen, D. Ni, B. Lei, and T. Wang, "Accurate segmentation of cervical cytoplasm and nuclei based on multiscale convolutional network and graph partitioning," *IEEE Transactions on Biomedical Engineering*, vol. 62, no. 10, pp. 2421-2433, 2015.

[17] R. Zhang, B. L. Osinski, T. J. Taxter, J. Perera, D. J. Lau, and A. A. Khan, "Adversarial deep learning for microsatellite instability prediction from histopathology slides."

[18] Y. Song *et al.*, "Accurate cervical cell segmentation from overlapping clumps in pap smear images," *IEEE transactions on medical imaging*, vol. 36, no. 1, pp. 288-300, 2017.

[19] C. D. Malon and E. Cosatto, "Classification of mitotic figures with convolutional neural networks and seeded blob features," *Journal of pathology informatics*, vol. 4, 2013.

[20] H. Wang *et al.*, "Cascaded ensemble of convolutional neural networks and handcrafted features for mitosis detection," in *Medical Imaging 2014: Digital Pathology*, 2014, vol. 9041, p. 90410B: International Society for Optics and Photonics.

[21] H. Hu, Q. Guan, S. Chen, Z. Ji, and L. Yao, "Detection and Recognition for Life State of Cell Cancer Using Two-Stage Cascade CNNs," *IEEE/ACM Transactions on Computational Biology and Bioinformatics*, 2017.

[22] A. A. Cruz-Roa, J. E. A. Ovalle, A. Madabhushi, and F. A. G. Osorio, "A deep learning architecture for image representation, visual interpretability and automated basal-cell carcinoma cancer detection," in *International Conference on Medical Image Computing and Computer-Assisted Intervention*, 2013, pp. 403-410: Springer.

[23] J. Xu *et al.*, "Stacked sparse autoencoder (SSAE) for nuclei detection on breast cancer histopathology images," *IEEE transactions on medical imaging*, vol. 35, no. 1, pp. 119-130, 2016.

[24] D. C. Cireşan, A. Giusti, L. M. Gambardella, and J. Schmidhuber, "Mitosis detection in breast cancer histology images with deep neural networks," in *International Conference on Medical Image Computing and Computer-assisted Intervention*, 2013, pp. 411-418: Springer.

[25] Y. Xie, X. Kong, F. Xing, F. Liu, H. Su, and L. Yang, "Deep voting: A robust approach toward nucleus localization in microscopy images," in *International Conference on Medical Image Computing and Computer-Assisted Intervention*, 2015, pp. 374-382: Springer.

[26] Y. Xie, F. Xing, X. Shi, X. Kong, H. Su, and L. Yang, "Efficient and robust cell detection: A structured regression approach," *Medical image analysis*, vol. 44, pp. 245-254, 2018.

[27] L. Ma *et al.*, "Deep learning based classification for head and neck cancer detection with hyperspectral imaging in an animal model," in *Medical Imaging 2017: Biomedical Applications in Molecular, Structural, and Functional Imaging*, 2017, vol. 10137, p. 101372G: International Society for Optics and Photonics.

[28] N. Coudray, A. L. Moreira, T. Sakellaropoulos, D. Fenyo, N. Razavian, and A. Tsirigos, "Classification and mutation prediction from non-small cell lung cancer histopathology images using deep learning," *bioRxiv*, p. 197574, 2017.

[29] L. Zhang, L. Lu, I. Nogues, R. M. Summers, S. Liu, and J. Yao, "DeepPap: Deep convolutional networks for cervical cell classification," *arXiv preprint arXiv:1801.08616*, 2018.

[30] V. Chandran, D. Kumar, P. Geetha, and R. Nidhya, "Deep Learning Neural Network with Semi supervised Segmentation for Predicting Retinal and Cancer Cell Diseased Images."

[31] K. Sirinukunwattana, S. E. A. Raza, Y.-W. Tsang, D. R. Snead, I. A. Cree, and N. M. Rajpoot, "Locality sensitive deep learning for detection and classification of nuclei in routine colon cancer histology images," *IEEE transactions on medical imaging*, vol. 35, no. 5, pp. 1196-1206, 2016.

[32] F. Xing, Y. Xie, and L. Yang, "An automatic learning-based framework for robust nucleus segmentation," *IEEE transactions on medical imaging*, vol. 35, no. 2, pp. 550-566, 2016.

[33] Y. Li, Y. Li, H. Kim, and S. Serikawa, "Active contour model-based segmentation algorithm for medical robots recognition," *Multimedia Tools and Applications*, vol. 77, no. 9, pp. 10485-10500, 2018.

[34] P. L. Narayanan, S. E. A. Raza, A. Dodson, B. Gusterson, M. Dowsett, and Y. Yuan, "DeepSDCS: Dissecting cancer proliferation heterogeneity in Ki67 digital whole slide images," *arXiv preprint arXiv:1806.10850*, 2018.

[35] M. Saha, C. Chakraborty, and D. Racoceanu, "Efficient deep learning model for mitosis detection using breast histopathology images," *Computerized Medical Imaging and Graphics*, vol. 64, pp. 29-40, 2018.

[36] M. Khoshdeli and B. Parvin, "Feature-Based Representation Improves Color Decomposition and Nuclear Detection Using a Convolutional Neural Network," *IEEE Transactions on Biomedical Engineering*, vol. 65, no. 3, pp. 625-634, 2018.

[37] O. Akin, Elnajjar, P., Heller. (Apr 27, 2017). *The Cancer Imaging Archive* Available: https://wiki.cancerimagingarchive.net/display/Public/TCGA-KIRC

[38] R. K. Yip, P. K. Tam, and D. N. Leung, "Modification of Hough transform for circles and ellipses detection using a 2-dimensional array," *Pattern recognition*, vol. 25, no. 9, pp. 1007-1022, 1992.

[39] A. Paul and D. P. Mukherjee, "Mitosis detection for invasive breast cancer grading in histopathological images," *IEEE Transactions on Image Processing*, vol. 24, no. 11, pp. 4041-4054, 2015.

[40] B. Korbar *et al.*, "Deep learning for classification of colorectal polyps on whole-slide images," *Journal of pathology informatics*, vol. 8, 2017.